Published in IET Intelligent Transport Systems
Received on 16th May 2014
Revised on 22nd August 2014
Accepted on 28th August 2014
doi: 10.1049/iet-its.2014.0101

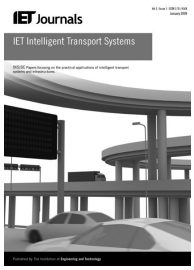

ISSN 1751-956X

Quantitative model of the driver's reaction time during daytime fog – application to a head up display-based advanced driver assistance system

Houssam Halmaoui[†] Karine Joulan[‡] Nicolas Hautière, Aurélien Cord, Roland Brémond

COSYS Department, Université Paris-Est, IFSTTAR, 14–20 boulevard Newton, Cité Descartes, Champs-sur-Marne, F-77 447 Marne-la-Vallée, France
[†]Present address: Cerema, Strasbourg, France
[‡]Present address: Continental, Toulouse, France
E-mail: nicolas.hautiere@ifsttar.fr

Abstract: Road accidents because of fog are relatively rare but their severity is greater and the risk of pile-up is higher. However, processing the images grabbed by cameras embedded in the vehicles can restore some visibility. Tarel *et al.* (2012) proposed to implement head up displays (HUD) to help drivers anticipate potential collisions by displaying dehazed images of the road scene. In the present study, three experiments have been designed to quantify the expected gain of such a system in terms of the driver's reaction time (RT). The first experiment compares the RT with and without dehazing, giving quantitative evidence that such an advanced driving assistance system (ADAS) may improve road safety. Then, based on a modified Piéron's law, a quantitative model is proposed, linking the RT to the target visibility (V_t), which can be computed from onboard camera images. Two additional experiments have been conducted, giving evidence that the proposed RT model, computed from V_t, is robust with respect to contextual cues, to contrast polarity and to population sample. The authors finally propose to use this predictive model to switch on/off the proposed HUD-based ADAS.

1 Introduction

A large proportion of road accidents occur under reduced visibility conditions, either because of rain, fog, night-time, visual masking or other environmental factors. Accidents because of fog are relatively rare but when they occur their severity is greater and the risk of pile-up is higher. The fog impairs driver visibility by reducing contrast exponentially with distance.

Several experiments have been conducted to compare the driver's perception of distance and speed in clear weather and in fog. Under such conditions, drivers are expected to reduce their speed. However, several studies have shown the opposite. Underestimating one's speed leads to overspeeding, and the denser the fog, the higher the speed [1]. Distance overestimation in fog may also contribute to the reduction of inter-vehicular distance: the distance overestimation is found between 25 and 50% in dense fog and around 6% in less dense fog [2]. More than half times the speed adjustment in fog does not allow a safe braking [3]. Drivers tend to follow too closely the front vehicle in fog, to keep it in sight [4]; meanwhile, impaired side vision may lead to line crossings [5].

The human factor is one of the main causes of road accidents, for example, lack of attention, lack of cognitive analysis or wrong manoeuvres [6]. The point of advanced driver assistance systems (ADAS) is to overcome driver failures and to improve safety and comfort by assisting the driver and providing information about the vehicle's environment. New systems seek to anticipate better to prevent accidents, using exteroceptive sensors allowing a better perception of the environment. Optical sensors such as cameras are becoming more prevalent because of their low cost, their small size and the richness of information provided. However, camera-based ADAS operate better under favourable weather and their performance may decrease drastically under reduced visibility conditions [7]. For instance, many image processing methods use descriptors that depend on colour and contrast in the image [8], which are degraded by atmospheric scattering in foggy weather.

While it is under low visibility that the driver most needs help, it is also then that the ADAS performance deteriorates. Fortunately, under foggy conditions, it is possible to detect and characterise fog by a vision algorithm, then to restore the signal at the output of the camera sensor, providing a better signal quality for the ADAS [9]. Together with improving ADAS performance in fog, the restored images with improved visibility may also be displayed to the driver with a head up display (HUD) to improve his perception of the road scene [10].

In the present paper, we evaluate the potential benefit of such a HUD-based ADAS, displaying restored images to the driver under foggy conditions. The gain of image dehazing is estimated in terms of reaction time (RT) and detection rate (DR) through psychophysical experiments,

using computer graphics (CG) images as stimuli. Then, a quantitative model is proposed to compute the expected RT gain online, from the target visibility computed from onboard camera images. Two more experiments assess the robustness of this model, so that we can propose to switch on/off the HUD depending on the expected RT gain, which can be computed online. The RT gain refers to the difference between the RT without and with image dehazing (in seconds).

The remainder of this paper is presented as follows. Some basic notions about fog and image dehazing are given in Section 2, together with the concepts of Piéron's law and of target visibility computations. The experiments are presented in Section 3, and the results in Section 4. These results are then discussed in Section 5 with respect to potential applications for a HUD-based ADAS.

2 Background

2.1 Dehazing of road images

Fog is made of small water droplets floating in the air that scatter the light. Before entering the driver's eyes, the light coming from a surface is scattered by this medium. During daytime, Koschmieder's model applies [11]

$$L = L_0 \mathrm{e}^{-kd} + L_\mathrm{s}(1 - \mathrm{e}^{-kd}) \tag{1}$$

where L is the luminance of an object as experienced by the driver, L_0 is its so-called intrinsic luminance (i.e. luminance at close range), L_s is the sky luminance, d is the distance between the object and the driver and k is the extinction coefficient of the atmosphere. The model includes two visual effects: the intrinsic luminance of an object decreases exponentially with the distance to the observer and the fog density, and the contribution of the atmospheric luminance increases exponentially with the distance.

According to the International Commission on Illumination, the meteorological visibility distance V_met is the distance at which the contrast of a black object is attenuated by 95% [12]. It can be related to the extinction coefficient k in (1) [7], leading to

$$V_\mathrm{met} = -\frac{\ln(0.05)}{k} \simeq \frac{3}{k} \tag{2}$$

Image dehazing needs to estimate L_0 from L, that is, to guess k, d and L_s in (1) [13–15, 10]. Assuming that the camera has a linear response, one can invert (1), so that the restoration formula is

$$L_0 = L\mathrm{e}^{kd} + L_\mathrm{s}(1 - \mathrm{e}^{kd}) \tag{3}$$

Equation (3) applies to the pixel's intensity, assuming that this intensity is proportional to L. In the following, image dehazing is computed with a previously published method [9], but other algorithms may apply as well [10].

2.2 Target visibility

Two distinct visibility concepts are considered in the following. We have seen that the meteorological visibility V_met is a conventional description of the fog extinction coefficient (see (2) and [12]). We will use it to design the CG images in our Experiments (see Section 3). The other visibility concept is the target visibility V_t: it rates to what extend a target is detected in a scene, when an observer looks at it. It is relevant in many contexts, including fog, dark, rain etc. Target visibility depends on human vision parameters such as the contrast sensitivity of the human eye.

A computational model of target visibility was proposed by Adrian for a uniform target on a uniform background [16, 17]. This model was developed from psychophysical data under various conditions [18], mainly for road lighting [19], and has also been considered in automotive lighting design. Unfortunately, this computational model is not suited for road images, because both the background and the car include texture, which makes it ambiguous to estimate the car and background luminance values.

Instead, we used an image processing estimation of the visibility [20], which was relevant for the target stimuli in all three experiments. This target visibility model, based on Barten's model of the human contrast sensitivity function [21], allowed computing the visibility from experimental data with good results under simple conditions [22]. It computes the visibility of the target's edges in an image; then, the visibility of a target is computed as the maximum visibility across the target's edges. A computed visibility of $V = 1$ means that there is 50% chance that an observer will see the target (if he looks at it). Note that V_t is not restricted between 0 and 1: for a simple uniform target on a uniform background, it is the ratio of the actual luminance contrast over the contrast needed for 50% chance of target detection.

2.3 Reaction time

Piéron's law is known to apply to any sensory channel (either visual, auditive etc.) and expresses the RT as a function of the stimulus intensity I

$$\mathrm{RT} = \beta I^{-\alpha} + t_0 \tag{4}$$

The shape of this function introduces three parameters: t_0 is the limit RT when the stimulus is obvious, α depends on the sensory modality and β depends on the experimental setup. If the stimulus is visible enough, the RT is close to a physiological RT (in our case, around 0.5 s). When the visibility decreased (as in fog), the RT is expected to increase.

However, Piéron's original law refers to a uniform stimulus on a uniform background [23, 24]. To cope with complex visual stimuli (a car, a pedestrian) and complex images (road environments), we were looking for a relation where the RT depends on the target visibility V_t

$$\mathrm{RT} = \beta V_\mathrm{t}^{-\alpha} + t_0 \tag{5}$$

For instance, we have seen that in fog, a car's contrast decreases as the distance increases. These two factors contribute to a lower visibility, which is expected to result in an increased RT with the fog intensity, and thus in more severe accidents.

2.4 Evaluation of a HUD-based ADAS

Tarel *et al*. [10] proposed that a HUD might improve the driver's visibility in foggy weather, by displaying processed images of the road scene, where fog is removed. They suggested that Piéron's law was relevant to estimate the expected gain of such an ADAS in terms of the driver's

doi: 10.1049/iet-its.2014.0101

RT. In the present paper, we address some questions which were left open in Tarel's paper:

- Piéron's law links the RT to the stimulus intensity. We argue that in the context of road images, intensity is not a relevant parameter, and we propose to use the target visibility instead (V_t), which can be computed from the images.
- We propose a quantitative model of RT as a function of V_t, so that RT can be computed online from road images (Section 4.2).
- This model is grounded on experimental data from a psychovisual experiment with a panel of participants (Section 4).
- This model may be useful in practical situation: we show that in dense fog, the expected RT gain is above 0.5 s.
- We give evidence of the model's robustness, in the sense that it is quite independent of the scene context, contrast polarity and, to some extent, observers panel (Section 4.3).
- From the above model, we propose that for a better acceptability of the HUD application, it should be turned off when the expected RT gain is below a given threshold.

3 Experiments

Three experiments have been conducted. The first one used realistic CG images of a road (see Fig. 1), produced by a dedicated software which could also simulate various fog densities [25]. These images were displayed either directly or after a dehazing image processing step [9]. The next two experiments used simpler conditions, with uniform discs as targets, and a uniform background. They were intended to check the validity/robustness of the results of Experiment 1 under more general conditions, without contextual information.

These experiments took place in a dark room with a surrounding luminance of 2.5 cd/m^2. A liquid crystal display (LCD) device was situated at 3 m in front of the participants. Its size was 60×44 cm^2, with a resolution of 2560×1440 pixels and a field of view of 11.4°. The displayed images were computed in luminance units (in cd/m^2) and displayed on the LCD thanks to a calibration model obtained from luminance measurements on this screen (Photometer Pritchard PR-880).

Each trial started with an auditive signal, followed by the background stimulus, during 1–3 s (this period was randomly chosen at each trial, to avoid a precise expectation of the stimulus onset by the participant). Then, the stimulus was displayed on the background, and the trial ended 5.5 s after the auditive signal. The participants were asked to report as soon as possible when they saw a target appearing on the display. The participant's responses were recorded with a gamepad, using the Presentation software [26] both to display the stimuli and record the responses.

The accuracy of the RT is lower than 1 ms, and RT longer than 2.5 s were not considered as relevant. Moreover, RT only makes sense when the target is detected, and some choice was needed about how to cope with targets which were sometimes detected, sometimes not. We decided not to use the RT data when the DR was below 50%, because this would mean that the available data is too sparse.

Fig. 1 *Sample stimuli from Experiment 1 (CG images)*
Top: without fog. Middle: with simulated fog. Bottom: after dehazing

Table 1 Simulated target distances d_1–d_5 for the stimuli in Experiment 1, for three fog densities, together with the associated meteorological visibility distances V_{met}

V_{met}	d_1	d_2	d_3	d_4	d_5
150	138	171	210	228	280
80	75	93	105	120	138
50	47	58	67	75	93

3.1 Experiment 1: foggy road environment

Thirty participants were involved in Experiment 1. CG cars were displayed on CG backgrounds, simulating road environments (see Fig. 1). The CG software simulated fog according to Koschmieder's law, taking into account the object's distance from the virtual camera [25]. Stimulus images were simulated for three fog densities, corresponding to meteorological visibility distances V_{met} set to 50, 80 and 150 m (see (2)). Two CG images were computed for each stimulus, with and without the target car. Then, the dehazing algorithm processed the resulting images.

For each fog density, the target cars were simulated at five distances, above and below the visibility distance, to capture the transition between visible and hidden targets (Table 1). Five target distances were used, and six repetitions for each fog condition: a baseline no-fog condition and three fog densities, both with the original image and after dehazing (i.e. seven fog conditions). For each stimulus, the detection performance was recorded, as well as the RT (when the target was detected). In all, each participant responded to 210 stimuli displayed in random order (5 distances × 6 repetitions × 7 fog conditions).

3.2 Experiment 2: simple dark target

The previous experiment used a specific road environment and a car as the target. We deemed that it was interesting to understand if the results from this experiment were dependent on this specific context, and on priors associated with a road environment. This is why we conducted a second experiment (Experiment 2) where all semantic information was removed, while luminance and contrast were the same as in Experiment 1. The same 30 participants as in Experiment 1 were involved in Experiment 2.

Instead of cars, the stimuli were discs, which are common psychophysics stimuli. We describe these discs as shapes seen through fog, at a distance, so that the visual performance in Experiment 2 could be associated to the driving situations in Experiment 1. Therefore the size and contrast of the discs were chosen to simulate objects with roughly the size of a car (2 m in width), set at a distance where one would usually see a car on the road, and with a colour consistent with the contrast attenuation in fog at this distance, according to Koschmieder's law (1). Fig. 2 shows three such stimuli corresponding to these disc-shaped objects in a foggy medium at 50, 80 and 150 m. The background luminance was set to $L_b = 150$ cd/m^2, whereas the intrinsic target luminance without fog was set to $L_0 = 0$ cd/m^2.

Owing to the lack of texture and other environmental cues, the task was slightly more difficult in Experiment 2 than in Experiment 1. Thus, the simulated target distances were chosen shorter in Experiment 2 (compare Table 2 with Table 1).

Stimulus images were simulated for three fog densities, corresponding to visibility distances V_{met} set to 50, 80 and 150 m, as in Experiment 1. For each fog density, the target was simulated at six distances, three above and three below the visibility distance, to capture the transition between visible and hidden targets (the disc sizes ranged from 0.25° to 2° of radius). The contrasts were negative, that is to say that the targets were darker than the background, just as cars in the fog. Each participant responded to 144 stimuli (3 fog densities, 6 target distances and 8 repetitions) displayed in random order.

3.3 Experiment 3: simple light target

The third experiment was a bit more challenging, in two respects. First, it is not straightforward that positive and negative contrasts are perceived equally well [16, 27], so we have recorded RTs with positive contrast targets, that is, targets which are lighter than their background. Second, people have idiosyncratic patterns for most aspects of their behaviour, which we have challenged by using a different panel of participants. They were aged from 18 to 59 years (mean = 32.8, SD = 8.9), with 7 women and 23 men. They were presented two disc sizes: 0.1° and 0.5° radius, with a uniform background luminance of 48.4 cd/m^2. For each disc, eight contrasts were used from 0.007 to 0.50, and each contrast was repeated eight times, so that each participant responded to 128 stimuli, presented in random order.

4 Results

4.1 Experiment 1: RT gain

Fig. 3 shows the mean RT as a function of the car distance. The left curves refer to a visibility distance when V_{met} = 50 m, the middle ones to $V_{met} = 80$ m and the right ones to $V_{met} = 150$ m. Each point is tagged with the associated DR. Dashed lines refer to foggy images, whereas continuous lines refer to dehazed images. The benefits of image dehazing also appears if we consider the RT gain, that is, the difference between RT without and with dehazing. It is clear that after dehazing, the RT is very close to what it

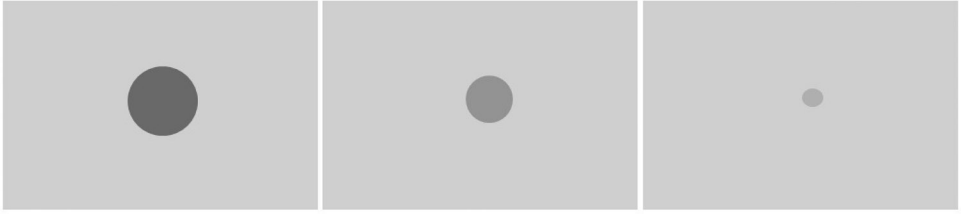

Fig. 2 *Samples of the stimuli displayed in Experiment 2, simulating a car-sized disc in a foggy medium, seen from 50 (left), 80 (middle) and 150 m (right)*

doi: 10.1049/iet-its.2014.0101

Table 2 Simulated target distances d_1–d_6 for the stimuli in Experiment 2, for three meteorological visibility distances V_{met}

V_{met}	d_1	d_2	d_3	d_4	d_5	d_6
150	75	105	138	171	210	228
80	42	57	75	93	105	120
50	28	37	47	58	67	75

would have been without fog (lower than 500 ms), showing that the gain under these conditions is close to optimal.

It was possible to describe our results in terms of target distance, which is a relevant parameter on the road. As an example, Table 3 shows the RT gain in moderate fog (V_{met} = 150 m), for various car distances. Considering a car around 200 m ahead on the road, we found that the RT gain with a HUD could be above 1 sec, which makes sense in terms of road safety.

Similarly, a RT gain around 1 sec was found for a car more than 100 m ahead in dense fog (V_{met} = 50 and 80 m).

It is also interesting to note that dehazing the images not only improves the RT, but also improves the DRs. Fig. 3 shows that the target DR can be quite low in fog (in Fig. 3, down to 9, 15 and 22% depending on the fog density), whereas the same DR is almost 100% after dehazing. This does not mean that the targets would not be detected at all without dehazing, but that they would be detected at shorter distances.

4.2 Experiment 1: model

The data were found consistent with a Piéron-like model (5), using the target visibility V_t estimated with a computer vision algorithm [20]. This is not an obvious result, because we have introduced the target visibility as the relevant intensity index, and we have proposed to use a computational account of this visibility, based on the human's contrast sensitivity function.

Based on (5), the data were fitted and the optimal values were found to be $\alpha = 1.29$, $\beta = 290$ and $t_0 = 0.455$ s [mean absolute error (MAE) = 77.5 ms], so that

$$\mathrm{RT} = 0.455 + 290 V_t^{-1.29} \tag{6}$$

is the best fit consistent with a Piéron-like model.

4.3 Experiments 2 and 3

The purpose of Experiments 2 and 3 was to control how sensitive the model was with respect to the CG images, to the target contrast polarity and to the sample population. Fig. 4 shows the relation between mean RT and target distance, for the three fog densities in Experiment 2. When the RT is considered as a function of the target visibility V_t, it is possible to estimate the corresponding parameters for Piéron's law. The same fitting as in Experiment 1 led to $\alpha = 1.39$ and to $\beta = 770$ (MAE = 101 ms). From Experiment 3, the best fit for a Pieron-like curve was found with $\alpha = 1.33$, $\beta = 330$ and $t_0 = 0.492$ s. The MAE was 17.2 ms, showing a very good consistency of the fitting. Note that the baseline RT is slightly different in Experiment 3 compared with Experiments 1 and 2, because these experiments did not share the same population sample. Gathering data from Experiments 2 and 3, the parameters which best matched the data in all conditions were $\alpha = 1.20$ and $\beta = 510$, leading to

$$\mathrm{RT} = 0.455 + 510 \times V_t^{-1.2} \tag{7}$$

with a MAE of 93.9 ms, which is satisfactory. Then, from (7), it was possible to look back at our data from Experiment 1, leading to a MAE = 213 ms, which is not so bad (compared with MAE = 77.5 ms using the model fitted to the data from Experiment 1 alone, see above).

Table 3 Expected RT gain using the HUD, as a function of the target distance, in medium-range fog (V_{met} = 150 m)

target distance, m	138	171	210	228
expected RT gain, s	0.057	0.069	0.754	1.366

5 Discussion

5.1 Main results

It was proposed that an image processing dehazing algorithm can be combined with a HUD system, and improve the RT of drivers in fog [10]. One benefit of such a system is that it is complementary to other onboard applications, and thus can be considered as a low cost application, depending on the available systems (onboard camera, image processing algorithms, HUD).

Three experiments were designed to rate the expected benefit from such a HUD application under foggy conditions, and to test whether a quantitative model would allow predicting this gain for foggy images. Our results give some evidence that a dehazing system has a strong potential impact in terms of road safety, thanks to the improved driver's RT (and DR) for the size targets of a car. Specifically, the main experiment (Experiment 1) allowed estimating the gain in RT using a HUD system in fog. We give evidence that the target visibility is a relevant parameter to estimate the RT from an image.

Considering an onboard application, the proposed system needs both the dehazing and the visibility computation to be performed in real time. Then, the RT gain can be computed online, for a given target. From this gain, an estimation of the road safety benefits (accident rate and severity) may be available, for instance from stopping distance models [28]. An onboard Intelligent Transportation System may decide to switch on or off the HUD.

The next two experiments consistently showed that the RT in front of simple images can be estimated with the same family of Piéron-like curves (5), and a quantitative model was proposed from these psychovisual experiments (7). Coming back to the first experiment, using CG stimuli close to those expected on the road, the proposed model appeared to be robust in terms of contextual priors, contrast polarity and observers panel.

5.2 RT, fog density and target distance

Provided that the target distance is available from some sensor (e.g. a lidar), it may be useful to combine Piéron's law and Koschmieder's law to estimate the RT as a function of a target distance. Some reasonable assumptions would be needed, concerning the target size and reference luminance L_0 to roughly simulate a dark car. However, Koschmieder's law (along with Adrian's target visibility model) deals with luminances and contrasts, which are not relevant variables for complex objects such as cars (which include internal contrast and texture), nor for complex backgrounds, such as

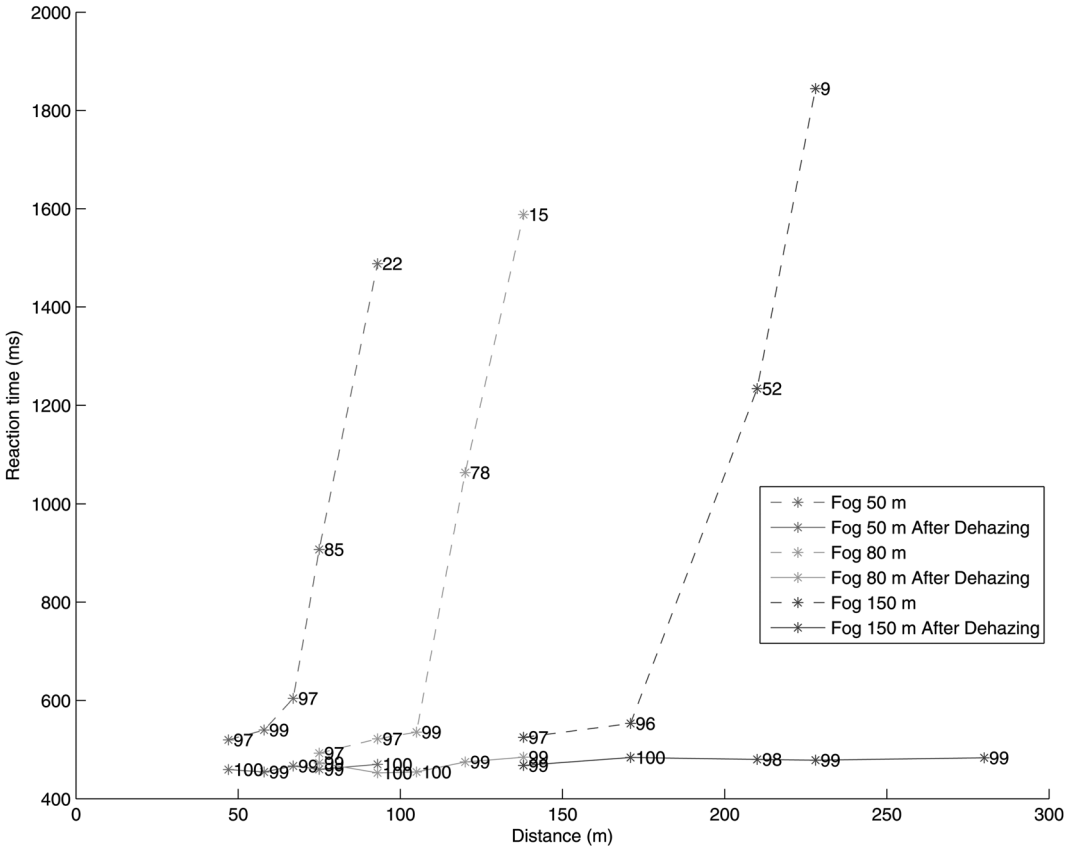

Fig. 3 *Mean RT as a function of the simulated target distance, for three simulated fog densities*

Left: $V_{met} = 50$ m, middle: $V_{met} = 80$ m and right: $V_{met} = 150$ m. Each point is tagged with the associated DR. Dashed lines refer to raw images, whereas continuous lines refer to images after dehazing

what is found on a road where the car's background is partly the road itself, and partly the landscape. This is not to suggest that contrast is not the relevant factor in terms of visual mechanisms, only that a practical definition of contrast is not available in the case of complex objects/backgrounds.

Arguably, some of the complexity is removed in foggy situations, with high spatial frequency information filtered out, making a car look like a target on a near-uniform foggy background, but this is expected to be very situation-dependent. We have tried, instead, to express the RT as a function of the target distance and fog density in Experiment 1, using our Piéron-like model. To do so, we estimated the target visibility V_t as a function of the distance for each of the three fog densities. Fortunately, a simple function appeared to roughly match the data

$$V_t \simeq A(k)e^{-Bd} \tag{8}$$

where $A(k)$ is a parameter which depends on the fog extinction coefficient k, $B = 0.035$ and d is the target distance. Table 4 gives estimated values of A, showing a good agreement with the data.

With this new function, it is possible to combine (5) and (8), leading to

$$\mathrm{RT} = \beta[A(k)e^{-0.035d}]^{-\alpha} + t_0 \tag{9}$$

and considering (6), we have

$$\mathrm{RT} = 290[A(k)e^{-0.035d}]^{-1.29} + 0.455 \tag{10}$$

We have only considered, in this study, three fog densities, so that we cannot propose a complete model of RT as a function of d. However, our results suggest that such a model would be useful and seems feasible, providing that more data are available: this way, an analytical model for $A(k)$ would replace the sample values given in Table 4.

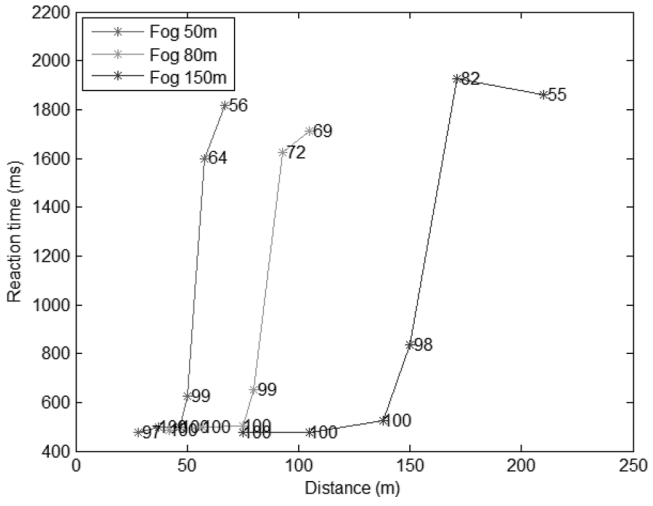

Fig. 4 *Mean RT as a function of the simulated target distance, for the three simulated fog densities in Experiment 2*

Left: $V_{met} = 50$ m; middle: $V_{met} = 80$ m; right: $V_{met} = 150$ m. Each point is tagged with the associated DR

doi: 10.1049/iet-its.2014.0101

Table 4 *A* values in (8), depending on the fog extinction coefficient *k*, and MAE

k	0.0600	0.0375	0.0200
A(*k*)	17	56	500
MAE	0.27	0.52	0.28

5.3 Limitations and future work

We are not at the end of the story, however, and a series of limitations apply to these results. For instance, the dehazing process which was used here was optimal, in the sense that the CG images did not include noise as in usual onboard road images (because of the sensor itself, the environment complexity, dust on the windshield etc.). Thus, the expected performance of a HUD may not reach the RT gain expected here. Using sensor images instead of CG images may contribute to estimate the true benefit of the proposed system, and further experiments on the road are also needed in the future to rate the level of visibility restored using such image processing on foggy images. One can expect that using road images, the RT gain will be shorter than what we found, and this gain should also depend on the dehazing algorithm itself. It would be interesting, in the future, to rate these algorithms in terms of target visibility restoration, in the sense of Joulan's algorithm [20].

Moreover, showing road images to a panel of observers instead of driving on the road leads to well-known biases [29]. Thus, our proposal should also be tested onboard a vehicle, using both a real-time dehazing algorithm, and a real-time computational model of target visibility, to compute (under foggy conditions) the RT gain of displaying detected targets with a HUD. An interesting test would be to implement such a system on a vehicles fleet, as suggested by Ward and Parkes [30], and to ask the drivers some complementary actions (including measuring their RT) to rate or to tune the algorithm and the decision model (whether or not to display the target vehicle with the HUD).

Camera limitations are also to be taken seriously. In the proposed HUD application, the RT can only be improved if the onboard camera actually sees something, for in dense fog it may happen that an object at a distance would not appear at all in the sensor image. In this case, the dehazing tool cannot see something which is not in the image raw data. One may suggest at this point that estimating the fog density [31] would help knowing the confidence range of the assistance system.

We did not address in this paper the HUD design, which may be critical to get the higher possible gain in terms of RT. This system is expected to make the relevant information easily available, without disturbing the driving task. Still, HUD is one among many ways to improve the visibility of targets on the road. For instance, a smartphone or tablet application may also give a visual feedback to the driver.

6 Acknowledgments

This study was partially funded by the ANR (French Research Agency) within the ICADAC project (6866C0210).

7 References

1 Snowden, R.J., Stimpson, N., Ruddle, R.A.: 'Speed perception fogs up as visibility drops', *Nature*, 1998, **392**, p. 450
2 Cavallo, V., Colomb, M., Dore, J.: 'The overestimation of headways in fog', *Recherche Transports Securite*, 2000, **2000**, (66), pp. 81–99
3 Sumner, R., Baguley, C., Burton, J.: 'Driving in fog on the M4'. Technical Report, TRL, 1977
4 Barham, P., Andreone, L., Toffetti, A., Bertolino, D., Eschler, J.: 'Changes to driving behaviour in conditions of reduced visibility when using an infrared vision support system: results of evaluations on a driving simulator'. Proc. Int. Conf. Traffic Transportation Psychology (ICTTP 2000), Bern, Switzerland, 2001, pp. 1–11
5 Tenkink, E.: 'Lane keeping and speed choice with restricted sight distances, road user behavior'. Proc. Second Int. Conf. on Road Safety, Groningen, Netherlands, 1988, pp. 169–177
6 Rumar, K.: 'The basic driver error: late detection', *Ergonomics*, 1990, **33**, pp. 1281–1290
7 Hautière, N., Tarel, J.-P., Aubert, D.: 'Mitigation of visibility loss for advanced camera-based driver assistance', *IEEE Trans. Intell. Transp. Syst.*, 2010, **11**, (2), pp. 474–484
8 Sun, Z., Bebis, G., Miller, R.: 'On-road vehicle detection: a review', *IEEE Trans. Pattern Anal. Mach. Intell.*, 2006, **28**, (5), pp. 694–711
9 Halmaoui, H., Cord, A., Hautiere, N.: 'Contrast restoration of road images taken in foggy weather'. 2011 IEEE Int. Conf. Computer Vision Workshops (ICCV Workshops), 2011, pp. 2057–2063
10 Tarel, J.-P., Hautière, N., Caraffa, L., Cord, A., Halmaoui, H., Gruyer, D.: 'Vision enhancement in homogeneous and heterogeneous fog', *IEEE Intell. Transp. Syst. Mag.*, 2012, **4**, (2), pp. 6–20
11 Middleton, W.: 'Vision through the atmosphere'. Geophysik II/ Geophysics II, 1957, pp. 254–287
12 CIE: Meteorological optical range, http://eilv.cie.co.at/term/772, 2012, International Commission on Illumination
13 Tan, R.T.: 'Visibility in bad weather from a single image'. Proc. IEEE Conf. Computer Vision and Pattern Recognition, 2008, pp. 1–8
14 He, K., Sun, J., Tang, X.: 'Single image haze removal using dark channel prior'. Proc. IEEE Conf. Computer Vision and Pattern Recognition, 2009, pp. 1956–1963
15 Tarel, J.-P., Hautière, N.: 'Fast visibility restoration from a single color or gray level image'. Proc. IEEE Int. Conf. Computer Vision, 2009, pp. 2201–2208
16 Adrian, W.: 'Visibility levels under night-time driving conditions', *J. Illum. Eng. Soc.*, 1987, **16**, (2), pp. 3–12
17 Adrian, W.: 'Visibility of targets: model for calculation', *Light. Res. Technol.*, 1989, **21**, (4), pp. 181–188
18 Blackwell, H.R.: 'Contrast thresholds of the human eye', *J. Opt. Soc. Am.*, 1946, **36**, (11), pp. 624–632
19 IESNA: 'Lighting Handbook, reference and application' (The Illumination Engineering Society of America, 2000)
20 Joulan, K., Hautière, N., Brémond, R.: 'A unified csf-based framework for edge detection and edge visibility'. Proc. CVPR Workshop on Biological Consistent Vision, 2011, pp. 21–26
21 Barten, P.: 'Contrast sensitivity of the human eye and its effects on image quality' (SPIE Optical Engineering Press, 1999)
22 Joulan, K., Brémond, R., Hautière, N.: 'Assessing an image processing model of edge visibility with a psycho-visual experiment', *Perception*, 2012, **41**, p. 241 (special issue, abstracts of the European Conference on Visual Perception)
23 Piéron, H.: 'Recherches sur les lois de variation des temps de latence sensorielle en fonction des intensités excitatrices', *L'année Psychologique*, 1913, **20**, pp. 17–96
24 Mansfield, R.J.W.: 'Latency functions in human vision', *Vis. Res.*, 1973, **13**, pp. 2219–2234
25 Gruyer, D., Grapinet, M., De Souza, P.: 'Modeling and validation of a new generic virtual optical sensor for ADAS prototyping'. IEEE Intelligent Vehicles Symposium, Alcala de Henares, Spain, 2012, pp. 969–974
26 NBS: 'Presentation software', http://www.neurobs.com/, 2013
27 Landwehr, K., Brendel, E., Hecht, H.: 'Luminance and contrast in visual perception of time to collision', *Vis. Res.*, 2013, **89**, pp. 18–23
28 Gallen, R., Hautière, N., Cord, A., Glaser, S.: 'Supporting drivers in keeping safe speed in adverse weather conditions by mitigating the risk level', *IEEE Trans. Intell. Transp. Syst.*, 2013, **99**, pp. 1–14
29 Mayeur, A., Brémond, R., Bastien, C.: 'Effects of the viewing context on peripheral target detection: implications for road lighting design', *Appl. Ergon.*, 2010, **41**, pp. 461–468
30 Ward, N.J., Parkes, A.M.: 'The effect of vision enhancement systems on driver peripheral visual performance'. Ergonomics and Safety of Intelligent Driver Interfaces, 1997, p. 239
31 Hautière, N., Tarel, J.-P., Lavenant, J., Aubert, D.: 'Automatic fog detection and estimation of visibility distance through use of an onboard camera', *Mach. Vis. Appl.*, 2006, **17**, (1), pp. 8–20